# Increased aerobic glycolysis is important for the motility of activated VSMC and inhibited by indirubin-3′-monoxime

**Elke H. Heiss**[a,*], **Daniel Schachner**[a], **Maddalena Donati**[b], **Christoph S. Grojer**[a], and **Verena M. Dirsch**[a]

[a]Department of Pharmacognosy, University of Vienna, Althanstrasse 14, 1090 Vienna, Austria

[b]Department of Pharmaceutical and Pharmacological Sciences, University of Padova, Via Marzolo, 5, 35131 Padova, Italy

## Abstract

Increased aerobic glycolysis is a recognized feature of multiple cellular phenotypes and offers a potential point for drug interference, as pursued by anti-tumor agents targeting the Warburg effect. This study aimed at examining the role of aerobic glycolysis for migration of vascular smooth muscle cells (VSMC) and its susceptibility to the small molecule indirubin-3′-monoxime (I3MO). Activation of VSMC with platelet-derived growth factor (PDGF) resulted in migration and increased glycolytic activity which was accompanied by an increased glucose uptake and hexokinase (HK) 2 expression. Inhibition of glycolysis or hexokinase by pharmacological agents or siRNA-mediated knockdown significantly reduced the migratory behavior in VSMC without affecting cell viability or early actin cytoskeleton rearrangement. I3MO, previously recognized as inhibitor of VSMC migration, was able to counteract the PDGF-activated increase in glycolysis and HK2 abundance. Activation of signal transducer and activator of transcription (STAT) 3 could be identified as crucial event in upregulation of HK2 and glycolytic activity in PDGF-stimulated VSMC and as point of interference for I3MO. I3MO did not inhibit hypoxia-inducible factor (HIF)1α-dependent transcription nor influence miRNA 143 levels, other potential regulators of HK2 levels. Overall, we demonstrate that increased aerobic glycolysis is an important factor for the motility of activated VSMC and that the anti-migratory property of I3MO may partly depend on impairment of glycolysis via a compromised STAT3/HK2 signaling axis.

## Keywords

VSMC; Migration; Aerobic glycolysis; Indirubin-3′ monoxime; Hexokinase

## 1 Introduction

Metabolic reprogramming, i.e. altered activity of selected energy production or biosynthetic pathways, has emerged as crucial player in determining the phenotype and signal transduction processes in a cell [1]. Already decades ago Otto Warburg noticed an increased rate of glycolysis in tumor cells despite the presence of oxygen [2]. This so-called Warburg effect, previously thought to be mainly caused by impaired respiration but now revised as metabolic program required to fulfill the needs of a proliferating tumor cell, has meanwhile consolidated as a hallmark of cancer and potential target for anticancer therapy [3,4]. Although still studied mainly in tumor models, a Warburg-like increased glycolytic rate also appears to be inherent to non-malignant cells such as activated macrophages or lymphocytes or regenerating skeletal muscle cells [5–7]. Moreover, in the vasculature inhibition of the glycolytic protein phosphofructokinase 2 (PFK2/PFKB3) in endothelial cells was sufficient to counteract their migration [8]. The role of bioenergetics in migration of vascular smooth muscle cells (VSMC), the cell type surrounding the endothelial monolayer in the vessel architecture, is little investigated. VSMC migration is prominently involved in important (patho)physiological processes such as wound healing, neoangiogenesis or vessel lumen constriction in the course of atherosclerosis or restenosis [9]. A bioenergetic facet would render VSMC migration an important (off) target to consider in the design of potential drugs affecting cellular energy metabolism.

Indirubin-3′-monoxime (I3MO) is a derivative of indirubin which is the active ingredient of the anti-leukemic traditional Chinese recipe Dangghui Longgui Wan and shows improved pharmacokinetics compared to its parent compound. Previous work from our group has extended the pharmacological research on I3MO from cancer to vascular biology and characterized I3MO as agent with triple vasoprotective bioactivity: it impairs VSMC proliferation and migration and counteracts inflammation by direct inhibition of monocyte 5-lipoxygenase [10–12]. Based on available data I3MO seems to also affect cellular energy metabolism by inhibition of glycogen synthase kinase (GSK) 3 beta [13], a key enzyme in glycogen metabolism, or by modulating mitochondrial function [14, 15]. Its role on VSMC bioenergetics has not been investigated until now.

Therefore we aimed at examining (i) whether migrating VSMC adopt a glycolytic phenotype, (ii) to what extent inhibition of glycolysis affects the motogenic activity of VSMC and (iii) whether the previously observed anti-migratory property of I3MO can be connected with changed bioenergetics.

## 2 Materials and methods

### 2.1 Materials and reagents

I3MO was purchased from Enzo Life Sciences (Lausen, Switzerland), the HIF 1α inhibitor BAY 87–2243 was from Selleck (via THP Medical Products, Vienna/Austria) and the STAT3 inhibitor SI 602 was ordered from Santa Cruz (Heidelberg, Germany). PDGF-BB was from Bachem (Weil am Rhein, Germany). Other chemicals unless stated otherwise were obtained from Sigma-Aldrich (Vienna, Austria). The anti-actin-antibody was obtained from MP Biomedicals (Solon, OH, USA), the anti-PFK1 and anti-HK1 antibodies were ordered

from Novus Biologicals (via THP Medical Products) and all other primary as well secondary antibodies were purchased from New England Biolabs (Heidelberg, Germany). All sterile cell culture material was from Greiner (Frickenhausen, Germany).

## 2.2 Cell culture

Primary rat aortic VSMC were purchased from Lonza (Braine-L'Alleud, Belgium). For experiments, they were thawed, cultivated in Dulbecco's modified essential medium (DMEM)–F12 (1:1) supplemented with 20% serum, 30 μg/mL gentamicin, and 15 ng/mL amphotericin B (Braine-L'Alleud, Belgium) and used between passage 4 and 15. Chinese hamster ovary cells (CHO-K1) were obtained from ATCC and also cultivated in DMEM supplemented with 10% FCS.

## 2.3 Wound healing assay (scratch assay)

The scratch assay was performed as previously described in [11].

## 2.4 Boyden chamber assay (transwell assay)

Serum- starved VSMC (0% serum, 24 h) were seeded at a density of 200,000 cells/well into pre-collagen I coated (5 μg/cm$^2$ rat collagen I; BD Biosciences, San Diego, CA, USA) cell culture inserts (BD Biosciences, San Diego, CA, USA). Chemotaxis was initiated by addition of 10 ng/ml PDGF (10.5 h)to the lower chamber. Cells were then stained with 8 μM Calcein- AM (Merck Millipore, Billerica, MA, USA) for 20 min. Cells on the upper side of the inserts (non-migrated cells) were completely scraped off with a Q-tip and washed away with PBS. Cells on the lower side of the inserts (migrated cells) were visualized under the microscope (Olympus Corporation, Tokyo, Japan) and photographed.

## 2.5 Determination of extracellular acidification and respiratory rates by extracellular flux analysis

VSMC were seeded in appropriate collagen-coated 24-well cell culture plates (from Seahorse Biosciences, Copenhagen, Denmark) at a cell density of $2 \times 10^4$ cells/well and treated as indicated. Cells were then kept in serum and glucose free assay medium (DMEM; pH 7.35–7.40) at 37 °C and ambient $CO_2$ for one hour before they were subjected to assessment of the extracellular acidification (ECAR in mpH/min) [and oxygen consumption rate (OCR in pmol $O_2$/min) if needed]. Appropriate test kits came from Seahorse Biosciences, were performed according to the manufacturer's instructions and analyzed on a Seahorse 24XFe extracellular flux analyzer and Wave software (www.seahorsebio.com) as described previously in [16,17]. Optimized inhibitor concentrations for VSMC were 3 μM oligomycin and 100 mM 2-deoxyglucose (2-DOG). Normalization to cell mass was routinely performed by crystal violet staining after the analysis in order to account for potential differences in cell number. Basal glycolytic activities were taken as readout and were calculated as follows: ECAR upon injection of glucose corrected for non-glycolytic acidification (ECAR in the presence of DOG).

### 2.6 Determination of extracellular lactate levels

VSMC were seeded in 24-well plates and treated as indicated. Then cells were incubated with Krebs Ringer HEPES Glucose (KRHG) buffer (50 mM HEPES, 136 mM NaCl, 23.5 mM KCl, 1.25 mM MgSO$_4$, 1.25 mM CaCl$_2$, 10 mM glucose and 0.1% BSA) for 1 h. Then an aliquot of the supernatant was mixed 1:1 with an AmplexRed/lactate oxidase (LO) solution (20 μM Amplex Red (Invitrogen), 0.5 mU/mL horseradish peroxidase (HRP), 0.1 U/mL LO in KRHG buffer) in order to monitor lactate levels. Lactate in the supernatant is oxidized by LO under stoichiometric production of H$_2$O$_2$ which in turn is used by HRP to oxidize Amplex Red to the fluorescent resorufin whose fluorescence is then read at ex 535 nm/em 590 nm in a TECAN Genios Pro fluorescence reader (TECAN Group Ltd., Männedorf, Switzerland) within the first 5 min of the reaction. Like this lactate levels can be quantified based on a standard curve with solutions of known lactate concentrations and referred to the protein concentration of the producing cells.

### 2.7 Determination of the cellular glucose uptake rate

The cellular glucose uptake rate was performed as previously described elsewhere [17].

### 2.8 Analysis of cell integrity

VSMC were treated as indicated before they were subjected to a trypan blue exclusion assay using an automated Vicell analyzer (Beckman Coulter) in order to assess cell integrity and viability.

### 2.9 siRNA-mediated knockdown of HK2, Nrf2 or STAT3

VSMC were seeded in appropriate dishes and grown to 60% confluency. Then cells were washed with Opti-MEM® (Gibco™, ThermoFisher Scientific, Vienna, Austria) and transfected with 60 to 200 nM siRNA- targeting rat HK-2, Nrf2 or STAT3 (*Silencer Select* predesigned from Ambion, Life Technologies, Vienna, Austria) or scrambled- siRNA (Ambion, Life Technologies, Vienna, Austria) using oligofectamine according to the manufacturer's instructions (Invitrogen, ThermoFisher Scientific, Vienna, Austria). After 5 h cells were given fresh medium and then used and prepared (i.e. reseeded and starved) for the planned assays.

### 2.10 Immunoblot

Extraction of proteins, electrophoresis, transfer, immunodetection and densitometric evaluation were performed as previously described [11].

### 2.11 F-actin staining by phalloidin-FITC

Coverslips were coated with 350 μg/ml rat collagen I solution in 0.02 N acetic acid (BD Bioscience Pharmingen, San Diego, CA, USA) for 2 h at room temperature. Coverslips were carefully washed twice with PBS, dried under sterile conditions and stored for up to 3 days at 4 °C. Cells were seeded at a density of $2 \times 10^5$ cells/well on to collagen I coated coverslips in 12-well plates for 24 h. Cells were then serum-starved for 48 h, pretreated with mannitol or DOG for 30 min and subsequently stimulated with PDGF-BB (10 ng/ml) for 1 h. Samples were briefly rinsed with PBS and extracted with a prewarmed solution of 0.25%

Triton X-100, 50% glutaraldehyde in a buffer containing 150 mM NaCl, 5 mM EGTA, 5 mM MgCl$_2$, 5 mM Glucose, 10 mM MES (2-($N$-Morpholino)-ethansulfonic acid), pH 6.1 for 1 min. Cells were postfixed with 1% glutaraldehyde in the same buffer at room temperature for 15 min, rinsed and washed with PBS for a few minutes. Coverslips were incubated with FITC-labeled phalloidin solution (New England Biolabs) for 30 min in a dark and humified chamber at room temperature. The coverslips were washed three times with PBS for 5 min and mounted on a glass slide using ProLong Gold antifade mounting medium (New England Biolabs, Heidelberg, Germany). After drying overnight in the dark the specimens were analyzed using a confocal fluorescence microscope (Leica Microsystems, Wetzlar, Germany).

### 2.12 Small G- protein pulldown assay

VSMC were seeded in 10 cm dishes and grown to 80% confluence. After 48 h of serum starvation cells were treated and stimulated as indicated, washed twice with ice-cold PBS and subsequently lysed. 20 μL of the lysate was taken away as input control. The remaining volume was subjected to a pulldown of activated rac and cdc42 using PAK-PBD sepharose beads (BioVision) and analyzed by an immunoblot for rac and cdc42, respectively.

### 2.13 HIF1α-dependent luciferase reporter gene assay

CHO cells were grown in 10 cm dishes to 70% confluency and transiently transfected with a HIF1α-dependent luciferase reporter construct (pGI3-EPO-HRE, [18]; kind gift from Thomas Kietzmann) and an EGFP expression plasmid (from ClonTech) using Lipofectamine Plus reagent according to the manufacturer's instructions. 16 h after transfection and recovery cells were harvested and re-seeded in 96-well plates ($5 \times 10^4$ cells/well) and serum starved till the next day. Then cells were treated as indicated for 8 h before the luminescence of the firefly luciferase and the fluorescence of EGFP were quantified on a GeniosPro plate reader (TECAN Group Ltd., Männedorf, Switzerland). The luminescence signals were normalized to the EGFP-derived fluorescence in order to account for differences in cell number and/or transfection efficiency.

### 2.14 Analysis of miR 143 levels

For this, $0.2 \times 10^6$ VSMCs between passage 4 and 8 were seeded into each well of six-well plates, starved for 48 h, treated as indicated and finally stimulated with PDGF-BB for up to 24 h. Total RNA, including microRNAs, was isolated from cellular samples with TRIzol reagent (Life Technologies Inc., Carlsbad, CA, USA) by applying a slightly modified protocol. 1-bromo-3-chloropropane was used instead of chloroform for phase separation and samples received an additional wash with 70% ethanol compared to the manufacturer's protocol. The isolated RNA was subjected to DNAse digestion (DNA-free kit, Life Technologies Inc) to increase sample purity. The quality of the isolated RNA was determined by UV-spectrophotometry (NanoDrop, Thermo Scientific, Willmington, DE, USA) and agarose electrophoresis. Reverse transcription into cDNA was performed with 500 ng RNA from each sample using the miScript II RT kit provided by QIAGEN (Hilden, Germany). Relative quantification of miR-143 levels via quantitative real-time PCR (qPCR) was performed on a LightCycler 480 instrument (Roche Diagnostics, Mannheim, Germany)

using the miScript SYBR green PCR kit and a miScript primer assay specific for miR-143 (both QIAGEN). U6 snRNA was used as a reference gene (primer assay from QIAGEN).

### 2.15 Statistics

At least three independent biological replicates of each experiment were performed. Error bars in the pictures represent the SD (standard deviation) of the mean. Statistical significance was determined by using Student's *t*-test or by one-way or two-way ANOVA followed by Bonferroni's or Dunnett's post test. All statistical analyses were done with GraphPad Prism. *P*-values <0.05 were considered as significant and are designated with * in the respective figures.

## 3 Results

### 3.1 PDGF triggers migration and increased glycolysis in primary rat aortic VSMC

VSMC were stimulated with platelet derived growth factor (PDGF) and served as model system to study the role of bioenergetics for VSMC migration. As reported previously (e.g. [12,19,20]), PDGF treatment of quiescent VSMC led to a significant increase in their migratory activity as seen in a scratch assay after 21 h (Fig. 1A). This period of time is shorter than the duration of one cell division cycle under the used cell culture conditions (i.e. $30 \pm 1.5$ h), excluding a marked contribution of proliferation to wound closure. Accordingly, a control experiment performed in the presence of the proliferation inhibitor mitomycin showed comparable wound closure (Supplemental Fig. 1). Moreover, PDGF triggered chemotaxis of VSMC in a Boyden chamber transwell assay, corroborating the pro-migratory impact of PDGF in VSMC (Fig. 1B). Using extracellular flux analysis and assessing the extracellular acidification rate (ECAR) showed an enhanced glycolytic rate in PDGF-treated VSMC (Fig. 1C). A consistent picture arose when extracellular lactate levels were monitored which excluded altered activity of membrane-residing proton pumps as culprit for the observed extracellular acidification (Fig. 1D). The unambiguous increase in glycolytic activity was accompanied by an enhanced cellular glucose uptake rate by activated VSMC (Fig. 1E) and only a slight reduction in the oxygen consumption rate (Supplemental Fig. 2). VSMC activation with PDGF furthermore led to a time-dependent induction of hexokinase (HK) 2 with no marked effect on HK1-, PFK1-, or PFK2 abundance (Fig. 1F), other rate controlling glycolytic enzymes. HKs catalyze the first step in glycolysis, i.e. phosphorylation of glucose to glucose-6-phosphat. HK occurs in four isoforms with partly cell-type specific expression profiles and HK2 being the principle regulated isoform, mainly expressed in myocytes and heavily involved in metabolic reprogramming.

### 3.2 Inhibition of glycolysis interferes with migration of VSMC

Subsequent examination of the migratory potential of activated VSMC when glycolysis was blunted intended to delineate a potential connection between bioenergetics and motility. Treatment with deoxyglucose (DOG), lonidamine- both glycolytic inhibitors [21,22]–, and siRNA mediated knockdown of HK2 (knockdown efficiency about 60% on protein level) consistently resulted in reduced PDGF-induced migration (Fig. 2A and B) suggesting that activated VSMC are indeed dependent on glycolysis in order to move. The used concentrations of DOG (5 mM for long-term and 30 mM for short term incubations) and

lonidamine (10 and 25 μM) successfully interfered with glycolytic activity (Fig. 2C) and did not cause any reduction in cell viability (Fig. 2D) which could possibly have contributed to the reduced motility of the cells. As glycolytic ATP was reported to be crucial for actin reorganization in endothelial cells [8], we had a look whether glycolysis inhibition also affects this crucial step for cell movement in VSMC. However, inhibition of glycolysis with DOG did not result in an obvious impairment of actin cytoskeleton reorganization. PDGF induced the formation of stress fibers, lamellipodia and filopodia in both control and DOG (30 mM)-treated cells as evident in the microscopic pictures after F-actin staining with FITC-phalloidin (Fig. 3A). This finding was confirmed by the indistinguishable activation of rac1 and cdc42, small G-proteins with a pivotal role in lamellipodia and filopodia formation [23,24], respectively, in control and DOG-treated VSMC upon PDGF exposure (Fig. 3B). Initially performed pilot experiments excluded an influence of DOG on basal rac or cdc42 activation. Unfortunately, rho A which is mainly involved in stress fiber formation could not successfully be immunoprecipitated from VSMC (as already experienced in [25]). Phosphorylation and activation of mitogen-activated protein (MAP) kinases, i.e. p38, ERK1/2 and JNK, or AKT kinase which are further events during actin cytoskeleton reorganization and migration (e.g. [26,27]) were not negatively affected by glycolysis inhibition, either (Fig. 3C). There was even a reproducible trend for enhanced and/or prolonged phosphorylation for some of those kinases in DOG-treated cells which could be explained by the redox sensitivity of the kinases and increased ROS production after DOG exposure. So far our findings showed that activated VSMC shift their energy metabolism towards an elevated glycolytic rate which is essential for their full motility but apparently not for early actin reorganization.

### 3.3 The anti-migratory small molecule I3MO abrogates increased glycolysis in activated VSMC

Intrigued by the revealed link between glycolysis and migration in VSMC we checked whether the antimigratory activity of the small molecule I3MO, recently uncovered in PDGF- or leukotriene-activated VSMC ([12]+ Fig. 4A), may carry a bioenergetic facet. Extracellular flux analysis indeed revealed an abrogated increase in glycolysis in activated VSMC treated with I3MO at 2.5 and 5 μM (Fig. 4B), concentrations that also negatively affect migration (Fig. 4A). The diminished glycolytic shift was in line with a reduction in PDGF-induced HK2 expression by I3MO (Fig. 4C). These findings indicate that I3MO is able to successfully overcome the PDGF-induced rise in glycolytic activity and to inhibit induction of HK2.

### 3.4 Impaired STAT3 signaling contribute to reduced HK2 expression and glycolysis in I3MO-treated activated VSMC

I3MO is a small molecule with pleiotropic actions and targets [28]. In PDGF-stimulated VSMC, I3MO acts as activator of Nrf2 — and inhibitor of STAT3 signaling by interfering with Y705 phosphorylation [11,12], respectively. We therefore examined the role of the two transcription factors for PDGF-induced HK2 expression and modulation by I3MO. Comparing VSMC with siRNA-depleted Nrf2 (knockdown by approximately 85%) to control cells revealed no difference in I3MO's capability of blunting PDGF-induced HK2 expression (Fig. 5A). Thus, the activation of Nrf2 by I3MO apparently does not directly

account for the observed reduction in HK2 expression. Experiments using the selective STAT3 inhibitor SI-602 demonstrated that STAT3 is heavily involved in PDGF-induced HK2 expression in VSMC (Fig. 5B). Consistent data were obtained when employing Stattic, another STAT3 inhibitor (data not shown). We aimed at corroborating this key finding for VSMC employing a siRNAmediated approach. Using a transient transfection protocol and two different concentrations of siRNA we could achieve knockdown efficiencies of STAT3 between 45 and 70% which were reflected in a diminished HK2 induction upon PDGF stimulation. This finding confirms the involvement of STAT3 in HK2 induction in VSMC (Fig. 5C) as already previously shown for cancer cells [29,30]. In line with the reduced HK2 induction inhibition or depletion of STAT3 also diminished the glycolytic rate and migratory activity of PDGF-activated VSMC as evident by extracellular flux analysis in the presence of SI-602 (Fig. 5D) and reduced scratch closure by STAT3-depleted cells (Fig. 5E), respectively. Induction of HK2 has also been linked with the activation of hypoxia-inducible factor (HIF-1α) signaling, also a downstream effect of activated STAT3, and with repression of microRNA 143 (e.g. [31–33]). We therefore examined the potential influence of I3MO on those two parameters. Also in PDGF-stimulated VSMC HK2 expression was reported to be HIF1α-dependent [34]. Accordingly, the HIF inhibitor BAY 87-2243 was able to significantly suppress HK2 levels in our test system (Fig. 6A). Reporter gene assays furthermore revealed that PDGF and cobalt chloride, a chemical inducer of hypoxia, led to an increase of HIF1α-dependent luciferase expression (Fig. 6B). However, I3MO activated HIF-1α-dependent reporter gene expression both under basal and PDGF- or cobalt-treated conditions (Fig. 6B) which disqualified HIF1a inhibition as responsible factor for the reduced HK2 expression by I3MO. Examination of miR 143 levels in VSMC disclosed an expected transient and time-dependent decrease in miR 143 upon activation with PDGF (Fig. 6C) which, however, was not significantly altered by I3MO (Fig. 6D). From these data we conclude that I3MO most likely interferes with STAT3- and not HIF-1α or miR 143 signaling in order to reduce HK2 expression and glycolysis in activated VSMC. Of note and in contrast to Y705, STAT3 phosphorylation at S727 which was found to markedly modulate mitochondrial function [35] was not affected by I3MO at 5 μM (Supplemental Fig. 3).

## 4 Discussion

The main new findings of this study are that (i) the glycolytic phenotype adopted by VSMC upon PDGF stimulation is crucial to provide them with a full migratory potential and (ii) I3MO abrogates this metabolic change and interferes with the STAT3-HK2 signaling axis.

Increased aerobic glycolysis appears as common cellular response to different cues and needs and is not restricted to cancer cells. This study showed that stimulation with the pro-migratory PDGF led to an elevated glycolytic rate in VSMC, in line with previous reports using PDGF as mitogen [36–38]. The raised glycolytic rate turned out as essential prerequisite for VSMC motility and was accompanied by an increased cellular glucose uptake and increased expression of HK2. HK2 is assigned not only a crucial role for boosting glycolysis but also for cellular survival. Its direct interaction with VDAC (voltage dependent anion channel), ANT (adenine nucleotide translocase) and cyclophilin D at the outer mitochondrial membrane prevents mitochondrial membrane transition pore opening and apoptosis [39,40]. It remains to be investigated whether HK2 in PDGF-activated VSMC

is bound to mitochondria and also plays a role in cytoprotection. Inhibition of HK activity by DOG and lonidamine and depletion of cells from HK2 by siRNA did not markedly affect cell viability under our experimental conditions, though.

Glycolytic inhibition by pharmacological or siRNA-mediated means significantly blunted migration which to our knowledge has not been reported before for VSMC. In contrast to endothelial cells, in which PFKB3 plays a major role in the metabolic control of motility, HK2 appeared as the predominantly modulated glycolytic protein when looking at abundance and thus remained focus of this study. However, changes in enzyme activity of other glycolytic enzymes, e.g. via post-translational modification, cannot be excluded in our system. Inhibition of glycolysis in activated VSMC did not obviously affect cytoskeletal actin reorganization. PDGF- activated cells phenotypically showed formation of stress fibers, lamelli-and filopodia, and on the molecular level activation of rac and cdc42 as well as phosphorylation of MAPK and AKT took place regardless of the presence of DOG (or I3MO, data not shown). Future studies need to pin down the step in the migratory cascade from polarization over protrusion and attachment to contraction which is affected by the inhibition of glycolysis in VSMC. Special attention should be given to changes in ATP levels (total or local at protrusions) and also to the question whether potential changes in the respiratory capacity contribute to VSMC motility.

I3MO, which we previously had identified as anti-migratory agent in VSMC due to activation of the Nrf2/heme oxygenase (HO)-1 axis, was for the first time revealed to significantly abrogate the PDGF-triggered increase in glycolytic activity and HK2 expression. Nrf2 knockout cells had been reported to show an elevated glycolytic rate [41], in line with the tested hypothesis that Nrf2 activation by I3MO accounted for reduced HK2 expression. However, knockdown of Nrf2 in VSMC showed that I3MO inhibited PDGF-induced HK2 expression regardless of Nrf2 presence. We therefore excluded pharmacological activation of Nrf2 by I3MO as major mechanism responsible for the observed reduction in HK2 abundance. It appeared that I3MO may inhibit VSMC migration by at least two mechanisms, (i) induction of the Nrf2/HO-1 axis as shown in [12] and (ii) an Nrf2-independent abrogation of HK2 induction. However, although without direct influence on HK2 expression, an activated Nrf2/HO-1 axis may still be involved in the dampened glycolytic activity. An increased HO-1 signaling has recently been shown to lead to diminished glycolysis in favor of the pentose phosphate pathway via altered PFKB3 methylation [42]. Whether this applies in I3MO-treated VSMC and could link together Nrf2 activation, reduced glycolysis and blunted migration warrants further investigation.

HK2 induction underlies a complex regulation including the control via STAT3, HIF-1α, and miR 143. Using selective STAT3 or HIF-1α inhibitors as well as siRNA-mediated depletion of STAT3 we could confirm that HK2 expression is dependent on both transcription factors in PDGF-stimulated VSMC. However, whereas I3MO markedly suppressed Y705 phosphorylation and activation of STAT3, it was not able to negatively interfere with HIF-1α signaling or alter changes in miR 143 levels in activated VSMC. In a HRE- dependent luciferase reporter gene assay, I3MO rather enhanced than inhibited the HIF1α-dependent signal, which is in line with a previous report on indirubins [43]. However, taking into account that HIF-1α is also a STAT3 target gene [35,44] and I3MO acts as an inhibitor of

STAT3 signaling in VSMC [10,11] this finding appears somewhat conflicting. But it needs to be noted that HIF1α signaling is not solely influenced by STAT3-dependent *de novo* synthesis, but also by other transcription factors triggering HIF1α expression, or by modulation of stability, posttranslational modification or transactivating potential of the protein [45] which could possibly provide a reconciling explanation.

## 5 Conclusion

Overall, we uncovered the importance of glycolysis for VSMC migration and an anti-glycolytic facet in the activity profile of I3MO via inhibition of the STAT3/HK2 axis. The latter may not only influence cellular motility but also contribute to the reported anti-proliferative and anti-inflammatory actions of I3MO since also proliferation and inflammation partly rely on an elevated glycolytic rate.

## Appendix A. Supplementary data

Refer to Web version on PubMed Central for supplementary material.

## Acknowledgements

## Abbreviations

| | |
|---|---|
| **Akt/PKB** | protein kinase B |
| **Bay** | BAY 87–2243 |
| **DOG** | deoxyglucose |
| **ERK** | extracellular-related signal kinase |
| **HIF** | hypoxia-inducible factor |
| **HK** | hexokinase |
| **HO** | heme oxygenase |
| **HRE** | HIF-responsive element |
| **HRP** | horseradish peroxidase |
| **I3MO** | indirubin-3′-monoxime |
| **JNK** | Jun-N-terminal kinase |
| **LO** | lactate oxidase |
| **Man** | mannitol |
| **MAPK** | mitogen activated protein kinase |

| **miR** | micro RNA |
| **Nrf2** | nuclear factor E2 related factor 2 |
| **PDGF** | platelet derived growth factor |
| **PFK** | phosphofructokinase |
| **SI** | STAT3 inhibitor 602 |
| **siRNA** | small interfering RNA |
| **STAT** | signal transducer and activator of transcription |
| **VSMC** | vascular smooth muscle cells |

## References

[1]. Metallo CM, Vander Heiden MG. Metabolism strikes back: metabolic flux regulates cell signaling. Genes Dev. 2010; 24:2717–2722. DOI: 10.1101/gad.2010510 [PubMed: 21159812]

[2]. Warburg O. On respiratory impairment in cancer cells. Science. 1956; 124:269–270. [PubMed: 13351639]

[3]. Chen X, Qian Y, Wu S. The Warburg effect: evolving interpretations of an established concept. Free Radic Biol Med. 2015; 79:253–263. DOI: 10.1016/j.freeradbiomed.2014.08.027 [PubMed: 25277420]

[4]. Yoshida GJ. Metabolic reprogramming: the emerging concept and associated therapeutic strategies. J Exp Clin Cancer Res. 2015; 34:111.doi: 10.1186/s13046-015-0221-y [PubMed: 26445347]

[5]. Palsson-McDermott EM, et al. Pyruvate kinase M2 regulates Hif-1alpha activity and IL-1beta induction and is a critical determinant of the Warburg effect in LPS-activated macrophages. Cell Metab. 2015; 21:65–80. DOI: 10.1016/j.cmet.2014.12.005 [PubMed: 25565206]

[6]. Ryall JG. Metabolic reprogramming as a novel regulator of skeletal muscle development and regeneration. FEBS J. 2013; 280:4004–4013. DOI: 10.1111/febs.12189 [PubMed: 23402377]

[7]. Donnelly RP, Finlay DK. Glucose, glycolysis and lymphocyte responses. Mol Immunol. 2015; doi: 10.1016/j.molimm.2015.07.034

[8]. Schoors S, et al. Partial and transient reduction of glycolysis by PFKFB3 blockade reduces pathological angiogenesis. Cell Metab. 2014; 19:37–48. DOI: 10.1016/j.cmet.2013.11.008 [PubMed: 24332967]

[9]. Louis SF, Zahradka P. Vascular smooth muscle cell motility: from migration to invasion. Exp Clin Cardiol. 2010; 15:e75–e85. [PubMed: 21264073]

[10]. Schwaiberger AV, et al. Indirubin-3′-monoxime blocks vascular smooth muscle cell proliferation by inhibition of signal transducer and activator of transcription 3 signaling and reduces neointima formation in vivo. Arterioscler Thromb Vasc Biol. 2010; 30:2475–2481. DOI: 10.1161/ATVBAHA.110.212654 [PubMed: 20847306]

[11]. Blazevic T, et al. 12/15-lipoxygenase contributes to platelet-derived growth factor-induced activation of signal transducer and activator of transcription 3. J Biol Chem. 2013; 288:35592–35603. DOI: 10.1074/jbc.M113.489013 [PubMed: 24165129]

[12]. Blazevic T, et al. Indirubin-3′-monoxime exerts a dual mode of inhibition towards leukotriene-mediated vascular smooth muscle cell migration. Cardiovasc Res. 2014; 101:522–532. DOI: 10.1093/cvr/cvt339 [PubMed: 24368834]

[13]. Leclerc S, et al. Indirubins inhibit glycogen synthase kinase-3 beta and CDK5/p25, two protein kinases involved in abnormal tau phosphorylation in Alzheimer's disease. A property common to most cyclin-dependent kinase inhibitors? J Biol Chem. 2001; 276:251–260. DOI: 10.1074/jbc.M002466200 [PubMed: 11013232]

[14]. Varela AT, et al. Indirubin-3′-oxime impairs mitochondrial oxidative phosphorylation and prevents mitochondrial permeability transition induction. Toxicol Appl Pharmacol. 2008; 233:179–185. DOI: 10.1016/j.taap.2008.08.005 [PubMed: 18786556]

[15]. Liao XM, Leung KN. Indirubin-3′-oxime induces mitochondrial dysfunction and triggers growth inhibition and cell cycle arrest in human neuroblastoma cells. Oncol Rep. 2013; 29:371–379. DOI: 10.3892/or.2012.2094 [PubMed: 23117445]

[16]. Zimmermann K, et al. Activated AMPK boosts the Nrf2/HO-1 signaling axis—a role for the unfolded protein response. Free Radic Biol Med. 2015; 88:417–426. DOI: 10.1016/j.freeradbiomed.2015.03.030 [PubMed: 25843659]

[17]. Heiss EH, et al. Glycolytic switch in response to betulinic acid in non-cancer cells. PLoS One. 2014; 9:e115683.doi: 10.1371/journal.pone.0115683 [PubMed: 25531780]

[18]. Kietzmann T, Cornesse Y, Brechtel K, Modaressi S, Jungermann K. Perivenous expression of the mRNA of the three hypoxia-inducible factor alpha-subunits, HIF1alpha, HIF2alpha and HIF3alpha, in rat liver. Biochem J. 2001; 354:531–537. [PubMed: 11237857]

[19]. Williams HC, et al. Role of coronin 1B in PDGF-induced migration of vascular smooth muscle cells. Circ Res. 2012; 111:56–65. DOI: 10.1161/CIRCRESAHA.111.255745 [PubMed: 22619279]

[20]. Marmur JD, Poon M, Rossikhina M, Taubman MB. Induction of PDGF-responsive genes in vascular smooth muscle. Implications for the early response to vessel injury. Circulation. 1992; 86:III53–III60. [PubMed: 1424052]

[21]. Bertoni JM. Competitive inhibition of rat brain hexokinase by 2-deoxyglucose, glu-cosamine, and metrizamide. J Neurochem. 1981; 37:1523–1528. [PubMed: 7334375]

[22]. Floridi A, et al. Enhancement of doxorubicin content by the antitumor drug lonidamine in resistant Ehrlich ascites tumor cells through modulation of energy metabolism. Biochem Pharmacol. 1998; 56:841–849. [PubMed: 9774146]

[23]. Charest PG, Firtel RA. Big roles for small GTPases in the control of directed cell movement. Biochem J. 2007; 401:377–390. DOI: 10.1042/BJ20061432 [PubMed: 17173542]

[24]. Marinkovic G, Heemskerk N, van Buul JD, de Waard V. The ins and outs of small GTPase Rac1 in the vasculature. J Pharmacol Exp Ther. 2015; 354:91–102. DOI: 10.1124/jpet.115.223610 [PubMed: 26036474]

[25]. Kumerz M, Heiss EH, Schachner D, Atanasov AG, Dirsch VM. Resveratrol inhibits migration and Rac1 activation in EGF- but not PDGF-activated vascular smooth muscle cells. Mol Nutr Food Res. 2011; 55:1230–1236. DOI: 10.1002/mnfr.201100309 [PubMed: 21732534]

[26]. Fegley AJ, Tanski WJ, Roztocil E, Davies MG. Sphingosine-1-phosphate stimulates smooth muscle cell migration through galpha(i)- and pi3-kinase-dependent p38(MAPK) activation. J Surg Res. 2003; 113:32–41. [PubMed: 12943808]

[27]. Chen Z, Cai Y, Zhang W, Liu X, Liu S. Astragaloside IV inhibits platelet-derived growth factor-BB-stimulated proliferation and migration of vascular smooth muscle cells via the inhibition of p38 MAPK signaling. Exp Ther Med. 2014; 8:1253–1258. DOI: 10.3892/etm.2014.1905 [PubMed: 25187834]

[28]. Blazevic T, et al. Indirubin and indirubin derivatives for counteracting proliferative diseases. Evid Based Complement Alternat Med. 2015; 2015:654098.doi: 10.1155/2015/654098 [PubMed: 26457112]

[29]. Liu YH, Wei XL, Hu GQ, Wang TX. Quinolone-indolone conjugate induces apoptosis by inhibiting the EGFR-STAT3-HK2 pathway in human cancer cells. Mol Med Rep. 2015; 12:2749–2756. DOI: 10.3892/mmr.2015.3716 [PubMed: 25937091]

[30]. Li Z, Li X, Wu S, Xue M, Chen W. Long non-coding RNA UCA1 promotes glycolysis by upregulating hexokinase 2 through the mTOR-STAT3/microRNA143 pathway. Cancer Sci. 2014; 105:951–955. DOI: 10.1111/cas.12461 [PubMed: 24890811]

[31]. Ackermann HW, et al. The species concept and its application to tailed phages. Arch Virol. 1992; 124:69–82. [PubMed: 1571021]

[32]. Zhou P, Chen WG, Li XW. MicroRNA-143 acts as a tumor suppressor by targeting hexokinase 2 in human prostate cancer. Am J Cancer Res. 2015; 5:2056–2063. [PubMed: 26269764]

[33]. Peschiaroli A, et al. miR-143 regulates hexokinase 2 expression in cancer cells. Oncogene. 2013; 32:797–802. DOI: 10.1038/onc.2012.100 [PubMed: 22469988]

[34]. Lambert CM, Roy M, Robitaille GA, Richard DE, Bonnet S. HIF-1 inhibition decreases systemic vascular remodelling diseases by promoting apoptosis through a hexokinase 2-dependent mechanism. Cardiovasc Res. 2010; 88:196–204. DOI: 10.1093/cvr/cvq152 [PubMed: 20498255]

[35]. Camporeale A, et al. STAT3 activities and energy metabolism: dangerous liaisons. Cancers (Basel). 2014; 6:1579–1596. DOI: 10.3390/cancers6031579 [PubMed: 25089666]

[36]. Werle M, et al. Metabolic control analysis of the Warburg-effect in proliferating vascular smooth muscle cells. J Biomed Sci. 2005; 12:827–834. DOI: 10.1007/s11373-005-9010-5 [PubMed: 16205843]

[37]. Chiong M, et al. Influence of glucose metabolism on vascular smooth muscle cell proliferation. Vasa. 2013; 42:8–16. DOI: 10.1024/0301-1526/a000243 [PubMed: 23385222]

[38]. Perez J, Hill BG, Benavides GA, Dranka BP, Darley-Usmar VM. Role of cellular bio-energetics in smooth muscle cell proliferation induced by platelet-derived growth factor. Biochem J. 2010; 428:255–267. DOI: 10.1042/BJ20100090 [PubMed: 20331438]

[39]. Wyatt E, et al. Regulation and cytoprotective role of hexokinase III. PLoS One. 2010; 5:e13823.doi: 10.1371/journal.pone.0013823 [PubMed: 21072205]

[40]. Roberts DJ, Miyamoto S. Hexokinase II integrates energy metabolism and cellular protection: Akting on mitochondria and TORCing to autophagy. Cell Death Differ. 2015; 22:248–257. DOI: 10.1038/cdd.2014.173 [PubMed: 25323588]

[41]. Ludtmann MH, Angelova PR, Zhang Y, Abramov AY, Dinkova-Kostova AT. Nrf2 affects the efficiency of mitochondrial fatty acid oxidation. Biochem J. 2014; 457:415–424. DOI: 10.1042/BJ20130863 [PubMed: 24206218]

[42]. Yamamoto T, et al. Reduced methylation of PFKFB3 in cancer cells shunts glucose towards the pentose phosphate pathway. Nat Commun. 2014; 5:3480.doi: 10.1038/ncomms4480 [PubMed: 24633012]

[43]. Schnitzer SE, Schmid T, Zhou J, Eisenbrand G, Brune B. Inhibition of GSK3beta by indirubins restores HIF-1alpha accumulation under prolonged periods of hypoxia/anoxia. FEBS Lett. 2005; 579:529–533. DOI: 10.1016/j.febslet.2004.12.023 [PubMed: 15642371]

[44]. Pedroza M, et al. STAT-3 contributes to pulmonary fibrosis through epithelial injury and fibroblast-myofibroblast differentiation. FASEB J. 2015; doi: 10.1096/fj.15-273953

[45]. Nagle DG, Zhou YD. Marine natural products as inhibitors of hypoxic signaling in tumors. Phytochem Rev. 2009; 8:415–429. DOI: 10.1007/s11101-009-9120-1 [PubMed: 20622986]
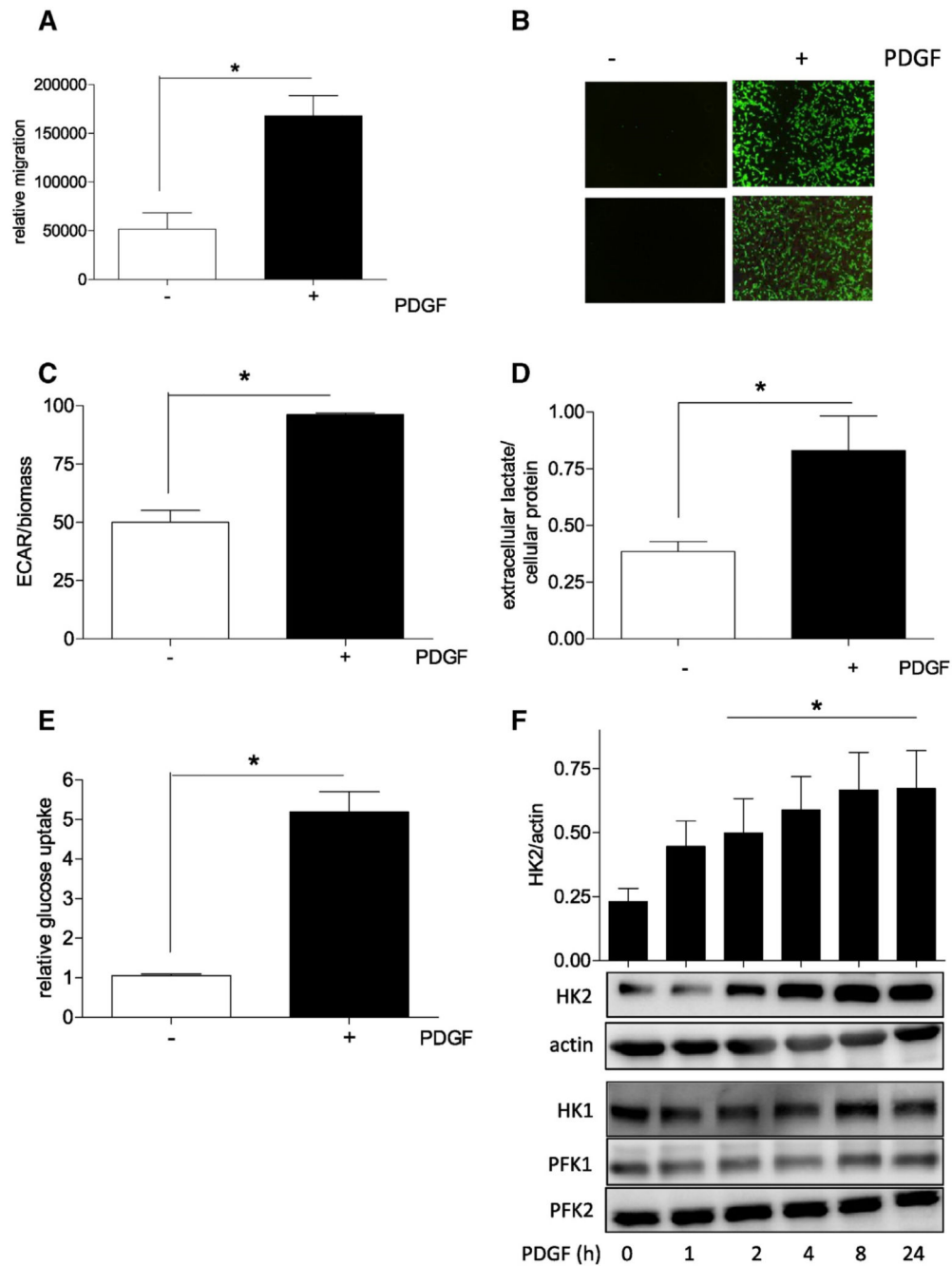
**Fig. 1.**
PDGF-triggered VSMC migration is accompanied by an increase in glycolytic activity, glucose uptake and hexokinase 2 expression. (A) Serum-deprived VSMCs were subjected to a wound healing (scratch) assay with or without stimulation with 10 ng/ml PDGF-BB for 21 h Graphs indicate relative values of wound closure as assessed by CellProfiler Software ($n$ = 3, mean + SD.; * $p$ < 0.05; Student's $t$-test). (B) Quiescent VSMC were subjected to a Boyden Chamber chemotaxis assay using 10 ng/mL PDGF (6 h) as chemotactic stimuli. Migrated cells were visualized by calcein-AM staining and photographed. Representative

pictures of three independent biological replicates with consistent results are shown. (C) Glycolytic activity in quiescent and PDGF-stimulated (6 h) VSMC was determined by extracellular flux analysis as described. The bar graph depicts compiled data of three independent experiments ($n = 3$, mean + SD.; * $p < 0.05$; Student's $t$-test) (D) Extracellular lactate accumulation was determined after PDGF stimulation (10 ng/mL, 6 h) by an enzyme-based fluorescence assay and subsequent correction for protein concentration. Bar graph depicts compiled data of three independent experiments ($n = 3$, mean + SD.; * $p < 0.05$; Student's $t$-test) (E) Cellular glucose uptake rate in quiescent and PDGF-stimulated (10 ng/mL; 6 h) VSMC was determined in an isotope-based assay. Bar graph depicts compiled data of three independent experiments ($n = 3$, mean + SD.; * $p < 0.05$; Student's $t$-test) (F) Quiescent VSMC were stimulated with PDGF (10 ng/mL) for the indicated periods of time before total cell extracts were subjected to western blot analyses for HK2, actin, HK1, PFK1 and 2. Bar graph depicts compiled densitometric data (HK2/actin) of three independent experiments ($n = 3$, mean + SD.; * $p < 0.05$; ANOVA, Dunnett vs unstimulated control).
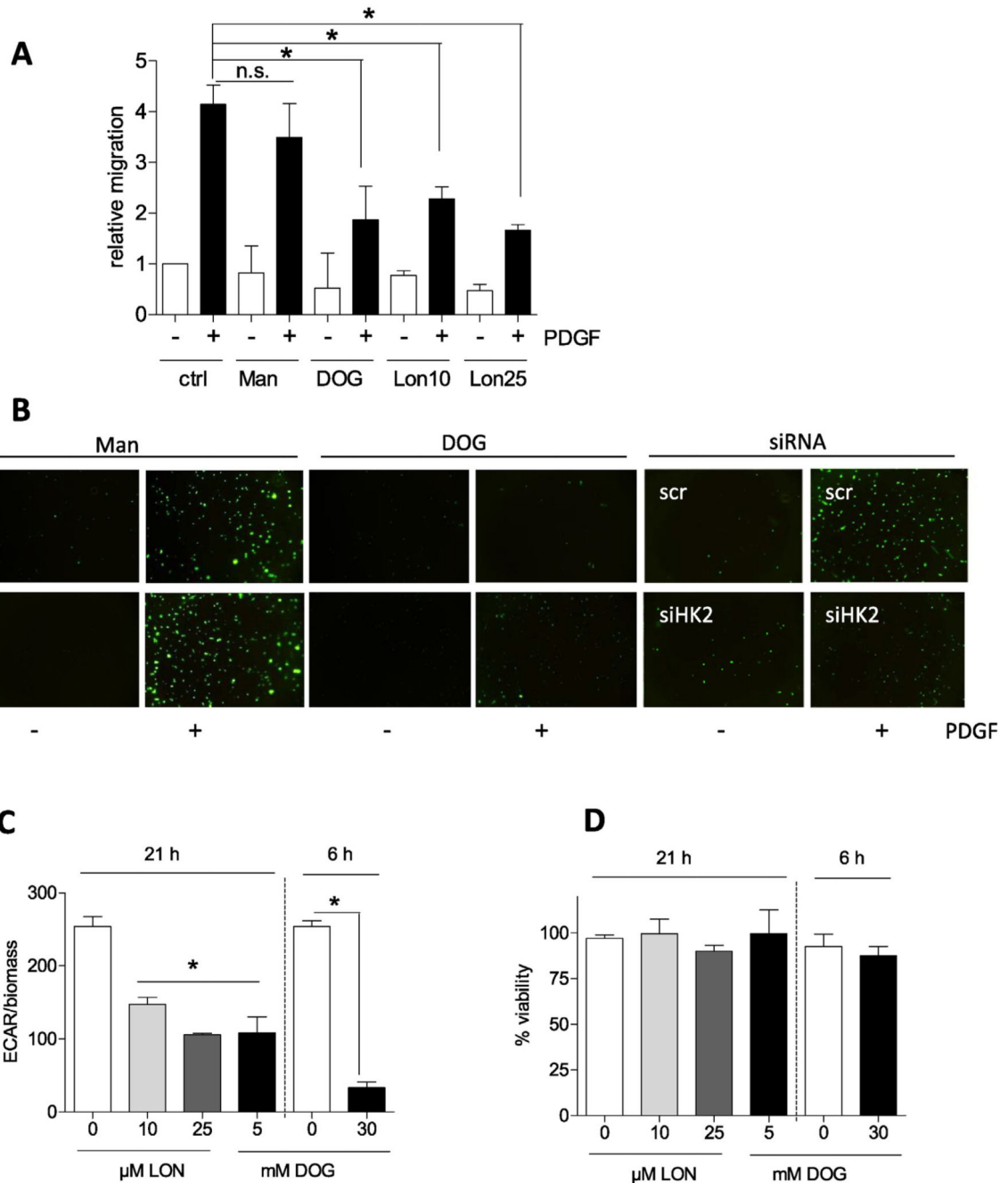
**Fig. 2.**

Inhibition of glycolysis overcomes PDGF-induced VSMC migration. (A) Serum-deprived VSMCs were pretreated with mannitol (Man; 5 mM; osmotic control), deoxyglucose (DOG, 5mM) and lonidamine (LON 10 and 25 μM) for 30 min as indicated and subjected to a wound healing (scratch) assay with or without stimulation with 10 ng/ml PDGF-BB for 21 h. Graphs indicate relative values of wound closure as assessed by CellProfiler Software ($n = 3$, mean + SD.; * $p < 0.05$; Student's $t$-test). B) Quiescent VSMC were pretreated as indicated (Mannitol (Man, ctrl), and deoxyglucose (DOG), 30 mM; or 200 nM siRNA)

subjected to a Boyden Chamber chemotaxis assay using 10 ng/mL PDGF (6 h) as chemotactic stimuli. Migrated cells were visualized by calcein-AM staining and photographed. Representative pictures of at least two independent biological replicates with consistent results are shown. (C) Glycolytic rate and (D) viability of VSMC were determined upon treatment with deoxyglucose (DOG) or lonidamine (LON) as indicated by extracellular flux analysis and trypan blue exclusion, respectively. ($n = 3$, mean + SD.; * $p < 0.05$; ANOVA, Dunnett vs untreated control).
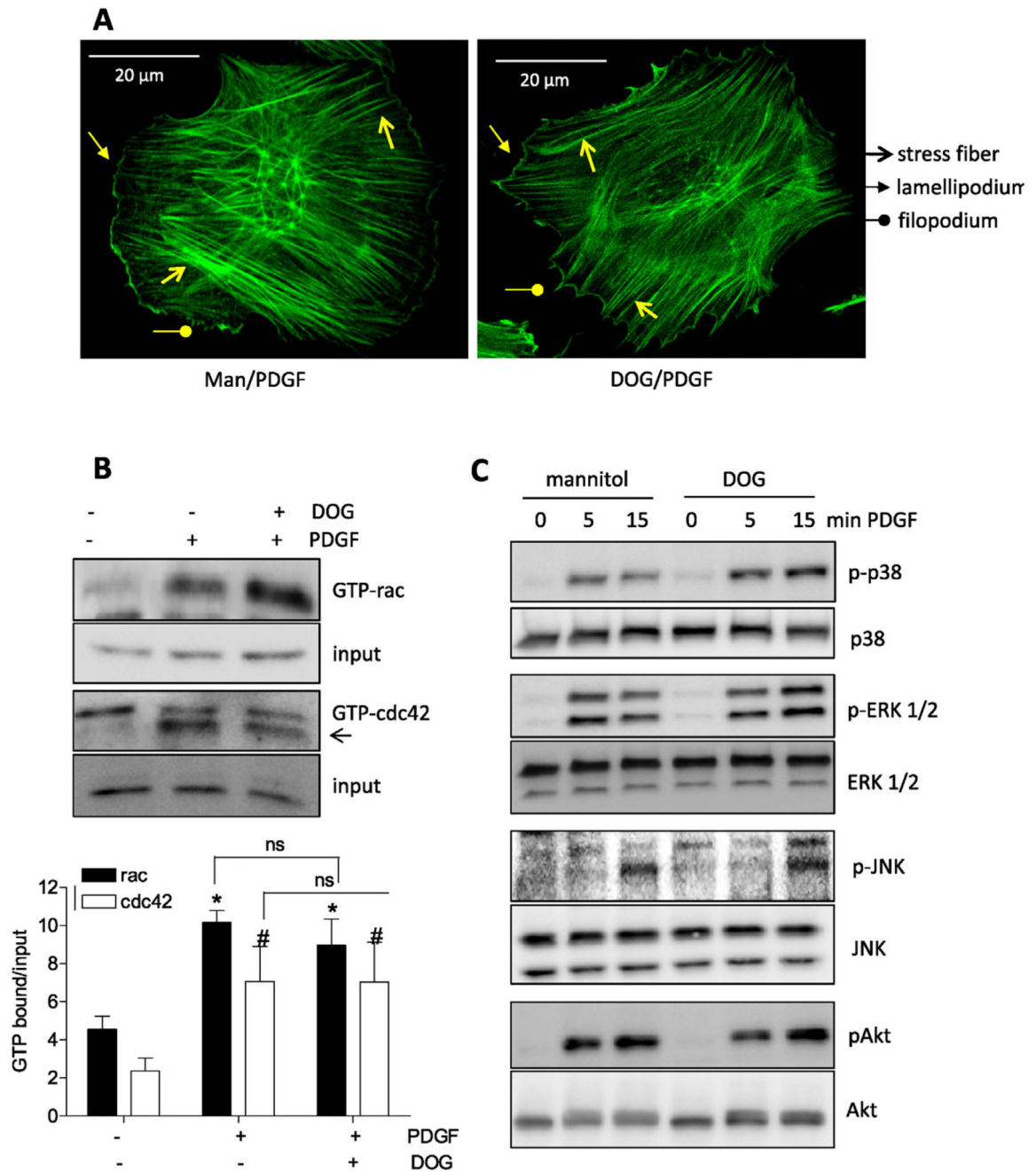
**A**



Man/PDGF

DOG/PDGF

→ stress fiber
→ lamellipodium
● filopodium

**B**



**C**



**Fig. 3.**
Inhibition of glycolysis does not interfere with early actin cytoskeleton reorganization. (A) Quiescent VSMC were stimulated with PDGF (10 ng/mL; 1 h) after 30 min pretreatment with mannitol (Man, 30 mM, osmotic control) or deoxyglucose (DOG, 30 mM). Cells were fixed, stained with FITC phalloidin and viewed under a confocal microscope. Stress fibers, lamelli –and filopodia are indicated with the appropriate arrows. (B) Quiescent VSMC were treated with 30 mM mannitol (−) or deoxyglucose (30 mM DOG) for 30 min as indicated before they were stimulated with PDGF (10 ng/mL) for 3 min. Lysates were then subjected

to pulldown of GTP bound ras and cdc42. An aliquot served as input control. Representative immunoblots from three independent experiments ae depicted. The bar graph shows compiled densitometric data from all performed experiments. ($n = 3$, mean + SD.; *, # $p < 0.05$; ANOVA, Dunnett (vs respective unstimulated control). (C) Quiescent VSMC were treated with 30 mM mannitol (−) or deoxyglucose (30 mM DOG) for 30 min as indicated before they were stimulated with PDGF (10 ng/mL) for 5 or 15 min. Lysates were then subjected to immunoblots analyses as indicated. Representative blots from three independent experiments are depicted.
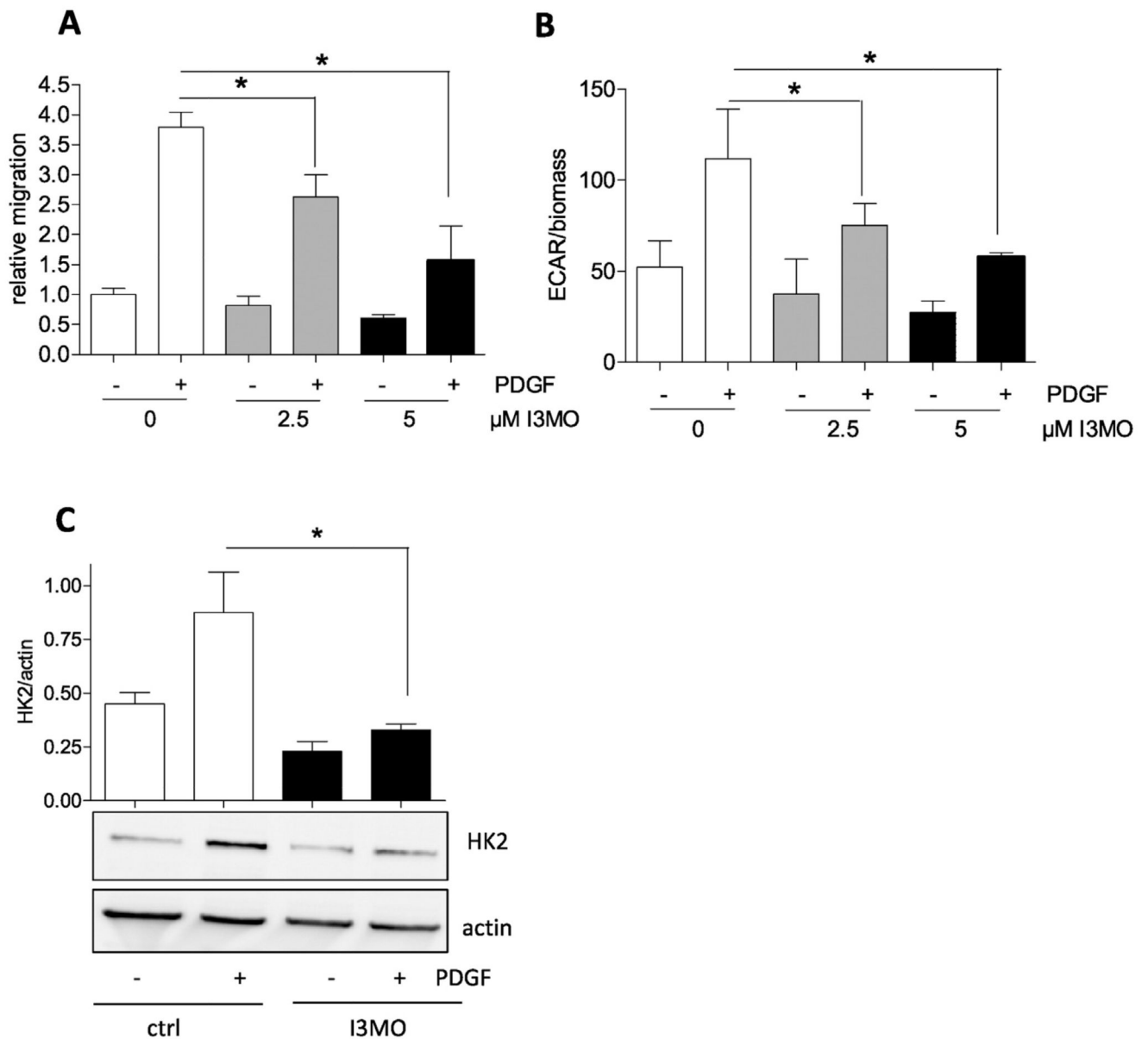
**Fig. 4.**

The antimigratory activity of I3MO is accompanied by a reduced glycolytic rate and diminished HK2 induction in PDGF-activated VSMC. (A) Serum-deprived VSMCs were subjected to a wound healing (scratch) assay with or without stimulation with 10 ng/ml PDGF-BB in the presence of 2.5 and 5 μM I3MO. Graphs indicate relative values of wound closure as assessed by CellProfiler Software ($n = 3$, mean + SD.; * $p < 0.05$; Student's $t$-test). (B) Glycolytic activity in quiescent and PDGF-stimulated (6 h) VSMC in the absence or presence of I3MO (2.5 and 5 μM) was determined by extracellular flux analysis as described. The bar graph depicts compiled data of three independent experiments ($n = 3$, mean + SD.; * $p < 0.05$; Student's $t$-test). (C) Serum-deprived VSMC were pretreated with 5 μM I3MO and then stimulated with PDGF (10 ng/mL) for 6 h. Total cell lysates were

subjected to immunoblot analysis for HK2 and actin. Representative blots from three independent experiments and compiled densitometric analysis are depicted ($n = 3$, mean + SD.; * $p < 0.05$; ANOVA, Bonferroni).
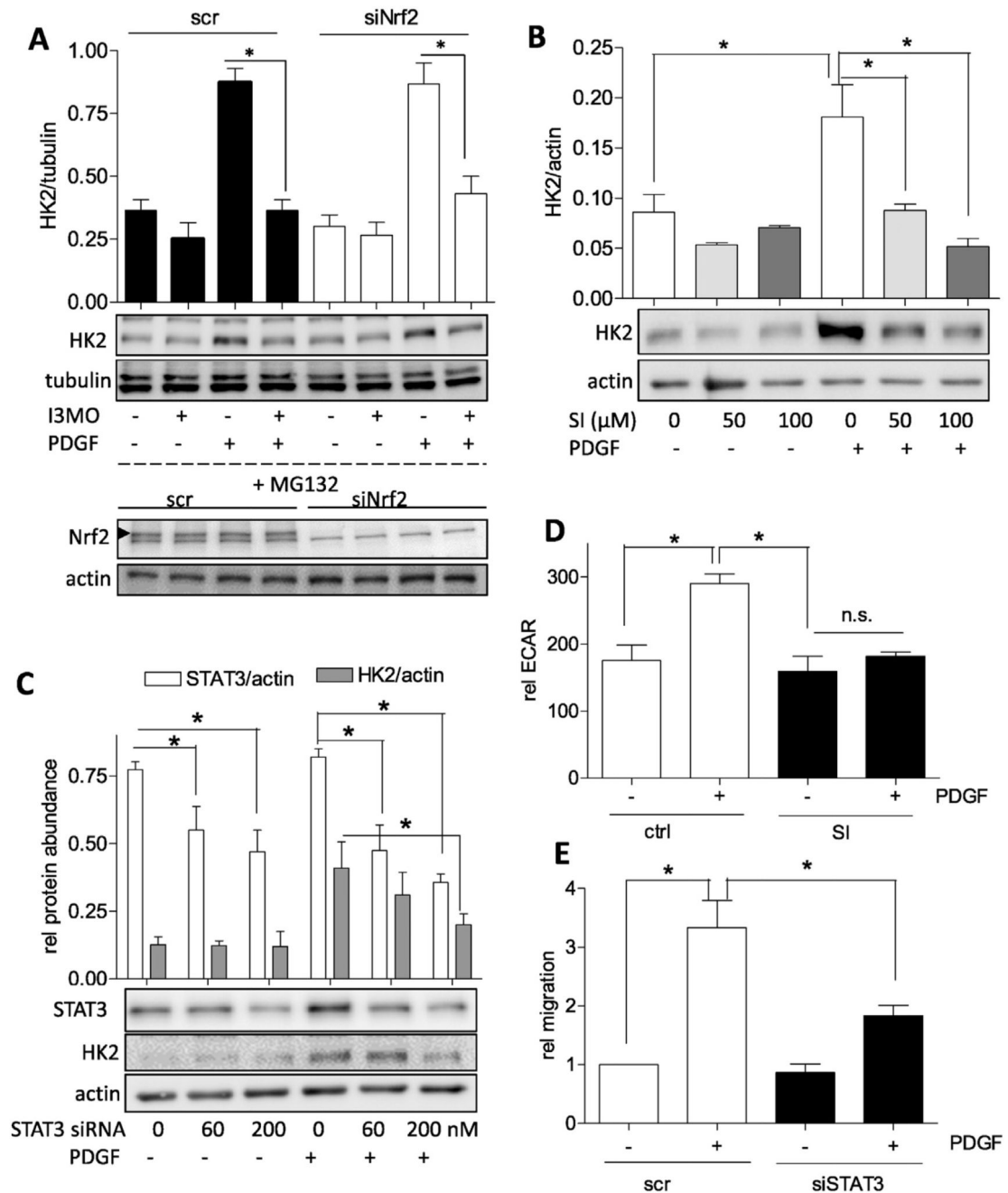
**Fig. 5.**
STAT3 positively regulates HK2 expression in PDGF stimulated VSMC and its inhibition is connected with decreased glycolysis and migration. (A) VSMC were transfected with 200 nM siRNA (scr or targeting Nrf2), after 24 h recovery starved for 18 h and then either treated with I3MO (5 μM)/PDGF as indicated for 8 h (upper panel) or with the proteasome inhibitor MG132 (10 μM) for 4 h (lower panel). Cells were lysed and total cell lysates subjected to western blot analysis for Nrf2 or actin and hexokinase or tubulin, respectively. Representative blots and compiled densitometric data from three independent experiments

are depicted. ($n = 3$, mean + SD.; * $p < 0.05$; ANOVA, Bonferroni). (B) Quiescent VSMC were pretreated with 50 and 100 μM of the STAT3 inhibitor SI-602 for 30 min and then exposed to PDGF (10 ng/mL) for 6 h. Total cell lysates were subjected to immunoblot analysis for HK2 and actin. Representative blots and compiled densitometric data are depicted. ($n = 3$, mean + SD.; * $p < 0.05$; ANOVA, Bonferroni). (C) VSMC were transfected with 0, 60 or 200 nM siRNA targeting STAT3 with a constant total siRNA concentration of 200 nM in all samples (filled up with scrambled siRNA where needed), starved and then treated with PDGF for 8 h. Cells were lysed and immunoblotted for STAT3, HK2 and actin. Representative blots and compiled densitometric data of three independent experiments are depicted. (D) Glycolytic activity in quiescent and PDGF-stimulated (6 h) VSMC in the presence and absence of the STAT3 inhibitor SI 602 (75 μM) was determined by extracellular flux analysis as described. The bar graph depicts compiled data of three independent experiments ($n = 3$, mean + SD.; * $p < 0.05$; Student's $t$-test). (E) Serum-deprived VSMCs that were either transfected with 200 nM scrambled siRNA or siRNA targeted versus STAT3 were subjected to a wound healing (scratch) assay with or without stimulation with 10 ng/ml PDGF-BB. Graphs indicate relative values of wound closure as assessed by CellProfiler Software ($n = 3$, mean + SD.; * $p < 0.05$; ANOVA, Bonferroni).
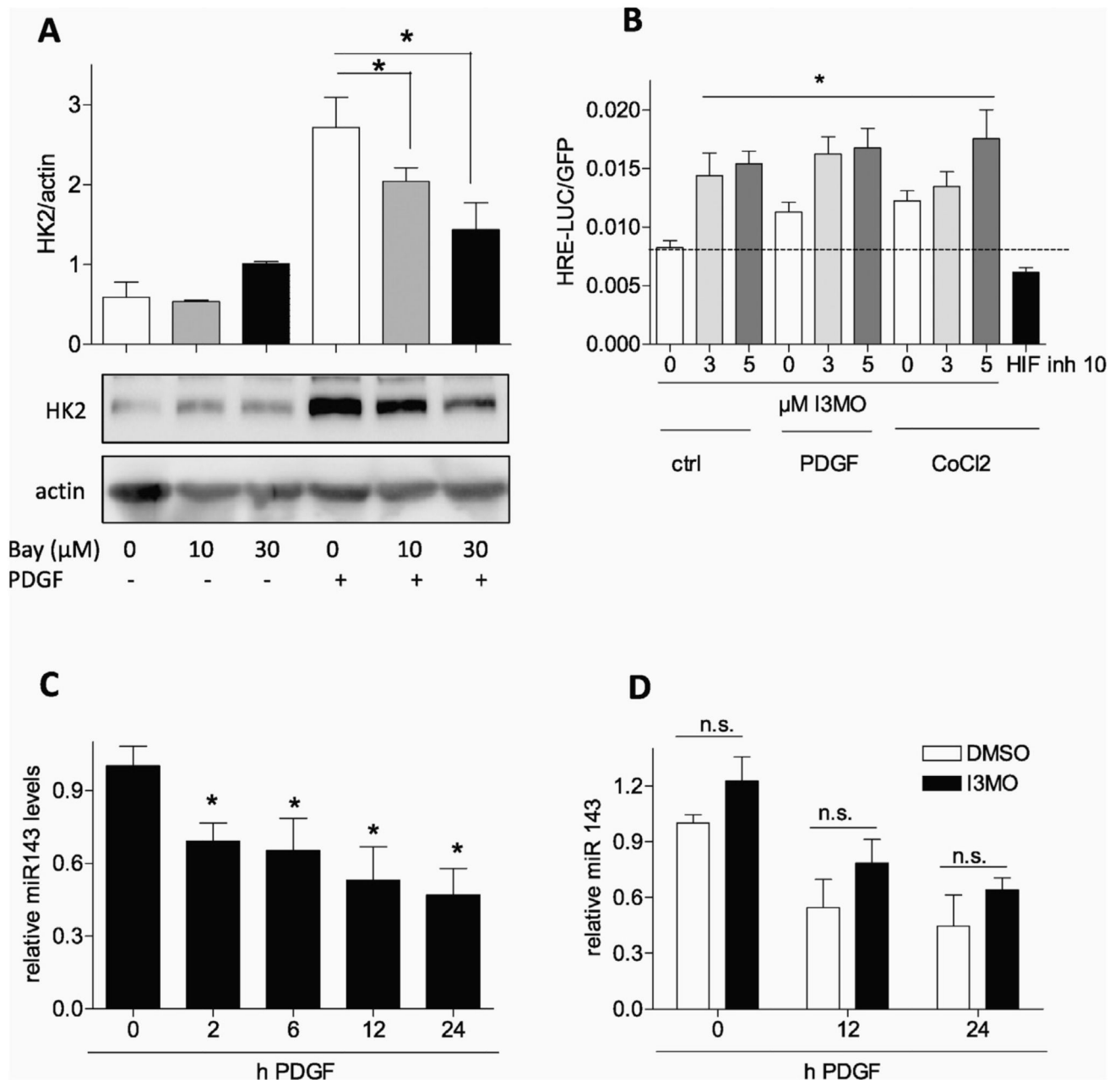
**Fig. 6.**
HIF1α-and miR143 signaling are not negatively influenced by I3MO. (A) Quiescent VSMC were pretreated with 10 or 30 μM HIF inhibitor BAY 87–2243 and then stimulated with PDGF (10 ng/mL) for 6 h. Total cell lysates were subjected to immunoblot analysis for HK2 and actin. Representative blots and compiled densitometric data from three independent experiments are depicted ($n = 3$, mean + SD.; * $p < 0.05$; ANOVA, Bonferroni). (B) CHO cells were transiently transfected with a HRE-LUC reporter gene and EGFP expression construct and serum-deprived. Cells were treated as indicated with I3MO (3 and 5 μM), PDGF (10 ng/mL) and $CoCl_2$ (200 μM) or HIF 1α inhibitor (10 μM) for 8 h before

luciferase activity was assessed and corrected for EGFP fluorescence. Bar graph depicts data from three independent experiments. ($n = 3$, mean + SD.; * $p < 0.05$; ANOVA, Bonferroni) (C) Quiescent VSMC were treated with PDGF for the indicated periods of time before levels of miRNA 143 were determined as described ($n = 5$, mean + SD; * $p < 0.05$; ANOVA, Dunnett vs unstimulated control). (D) Quiescent VSMC were pretreated with DMSO or I3MO for 30 min prior to PDGF stimulation for the indicated periods of time. Then relative miRNA 143 levels were determined as described. ($n$ 6, mean + SD, n.s. $p > 0.05$).